APPLICATION ARTICLE

DNA release from plant tissue using focused ultrasound extraction (FUSE)

Alexia Stettinius[1] | Hal Holmes[1,2] | Qian Zhang[3] | Isabelle Mehochko[1] |
Misa Winters[2] | Ruby Hutchison[1] | Adam Maxwell[4] | Jason Holliday[3] |
Eli Vlaisavljevich[1]

[1]Department of Biomedical Engineering and Mechanics, Virginia Polytechnic Institute and State University, Blacksburg, Virginia, USA

[2]Conservation X Labs, Seattle, Washington, USA

[3]Department of Forest Resources and Environmental Conservation, Virginia Polytechnic Institute and State University, Blacksburg, Virginia, USA

[4]Department of Urology, University of Washington, Seattle, Washington, USA

Correspondence
Alexia Stettinius, Department of Biomedical Engineering and Mechanics, Virginia Polytechnic Institute and State University, 325 Stanger Street, Room 349 Kelly Hall, Blacksburg, Virginia 24061, USA.
Email: astettinius@vt.edu

Abstract

Premise: Sample preparation in genomics is a critical step that is often overlooked in molecular workflows and impacts the success of downstream genetic applications. This study explores the use of a recently developed focused ultrasound extraction (FUSE) technique to enable the rapid release of DNA from plant tissues for genetic analysis.

Methods: FUSE generates a dense acoustic cavitation bubble cloud that pulverizes targeted tissue into acellular debris. This technique was applied to leaf samples of American chestnut (*Castanea dentata*), tulip poplar (*Liriodendron tulipifera*), red maple (*Acer rubrum*), and chestnut oak (*Quercus montana*).

Results: We observed that FUSE can extract high quantities of DNA in 9–15 min, compared to the 30 min required for control DNA extraction methods. FUSE extracted DNA quantities of 24.33 ± 6.51 ng/mg and 35.32 ± 9.21 ng/mg from American chestnut and red maple, respectively, while control methods yielded 6.22 ± 0.87 ng/mg and 11.51 ± 1.95 ng/mg, respectively. The quality of the DNA released by FUSE allowed for successful amplification and next-generation sequencing.

Discussion: These results indicate that FUSE can improve DNA extraction efficiency for leaf tissues. Continued development of this technology aims to adapt to field-deployable systems to increase the cataloging of genetic biodiversity, particularly in low-resource biodiversity hotspots.

KEYWORDS
DNA extraction, focused ultrasound, genomics, plant genetics

Over the past two decades, developments in genome sequencing technologies have enabled researchers to provide an unprecedented scope and depth of genetic information. Emerging technologies have equipped researchers with the tools to perform DNA and RNA sequencing in the field (Jain et al., 2016), which could allow for new genetics research to be carried out by non-scientists in a variety of settings that had not previously been feasible (Rachmayanti et al., 2009; Niemz et al., 2011; Dormontt et al., 2015). However, despite these technological advancements, many plant species are poorly represented in genetic databases, which limits the applicability of field-deployable sequencing platforms (Liu et al., 2021). For example, of the nearly 400,000 unique plant species estimated to exist, only 600 have nearly complete genome coverage and assembly (Kersey, 2019). With such limited coverage of plant taxa, it is likely that many opportunities for new uses of undiscovered traits unique to species have gone unnoticed, and increasing extinction rates may cause the loss of some of these opportunities. Sequencing plant

genomes is also essential for utilizing genetic resources in breeding programs (Halewood et al., 2018), conserving plant species (Finch et al., 2019, 2020), and understanding their role in ecosystem function (CBOL Plant Working Group, 2009; Holliday et al., 2017; Cornwell et al., 2019) and phylogenetic studies (Small et al., 1998). Therefore, the continued expansion of plant genetic databases is essential to spur discovery, drive innovation, and protect crucial resources.

A robust DNA extraction protocol that yields DNA of sufficient concentration and purity is essential for success in genotyping and sequencing applications. In plants, the release of viable DNA is hindered by tough tissue matrices that are resistant to mechanical breakdown, the presence of polysaccharide-rich cell walls, and many inhibitory compounds such as polyphenolic metabolites (Porebski et al., 1997; Rachmayanti et al., 2009; Särkinen et al., 2012). To combat these challenges, tissue pulverization using benchtop tools, such as a mixer mill, or a mortar and pestle under liquid nitrogen, is used in conjunction with plant cell lysis and purification protocols. Plant DNA extraction is often cumbersome, and despite specialized tissue breakdown strategies, releasing DNA suitable for genomic analysis is challenging for many sample types (Jiao et al., 2018). Additionally, current plant DNA extraction techniques require an advanced laboratory (Buser et al., 2016). With a growing need for field-deployable species identification tools for biodiversity conservation, the ability to translate DNA extraction protocols to the field is becoming increasingly important (Dormontt et al., 2015). The simplification of DNA extraction could be pivotal in conservation efforts where researchers must rapidly and inexpensively prepare samples from biodiversity hotspots, which are often remote and far removed from centralized laboratories (Pironon et al., 2020).

Our group has recently developed a technology capable of accelerating and simplifying the DNA extraction workflow, termed focused ultrasound extraction (FUSE), to address sample preparation and DNA extraction challenges. FUSE has previously demonstrated its capacity to rapidly release DNA from Atlantic salmon muscle tissue samples with intense cavitation clouds generated by focused ultrasonic transducers (Holmes et al., 2020). This technology employs dense acoustic cavitation bubble clouds similar to those used in histotripsy, a non-invasive focused ultrasound therapy currently being developed for medical applications (Bader et al., 2019; Xu et al., 2021). During FUSE, the rapid expansion and violent collapse of the cavitation microbubbles induce high stress on the target tissue, which causes mechanical disintegration and results in an acellular tissue lysate (Vlaisavljevich et al., 2016; Mancia et al., 2017). The tissue lysate is then collected, and the released DNA is purified for downstream analyses. This process differs from conventional extraction methods that require mechanical tissue disruption followed by incubation periods varying from 10 min to 1 h, depending on the plant tissue, before DNA collection and purification (Figure 1).

Here, we test the efficacy of FUSE with leaf tissue by (1) determining the feasibility of leaf tissue breakdown, (2) measuring the DNA yield, (3) amplifying the released DNA with PCR to verify DNA quality, and (4) sequencing the resultant DNA libraries to validate the utility of FUSE in whole-genome sequencing applications. While our ultimate goal is to adapt FUSE to low-cost and field-deployable systems to enable rapid sample processing and DNA extraction from various sample types, here we address the feasibility of FUSE for DNA release from leaf tissue in a laboratory setting using prototype transducers and custom acoustically transparent sample holders. We hypothesize that FUSE can pulverize leaf tissue and yield significant quantities of DNA with a quality suitable for PCR amplification and next-generation sequencing. If successful, FUSE could streamline leaf DNA extraction workflows to improve standard laboratory practices. Further technology development could allow the miniaturization of the FUSE system to bring this technology to the field to expand the scope of opportunities.

MATERIALS AND METHODS

Plant materials

To demonstrate the ability of FUSE to rapidly provide amplifiable DNA fragments for genetic analysis, we used fresh leaf samples collected from American chestnut (*Castanea dentata* (Marshall) Borkh.), tulip poplar (*Liriodendron tulipifera* L.), red maple (*Acer rubrum* L.), and chestnut oak (*Quercus montana* Willd.) trees found on the Virginia Tech campus in Blacksburg, Virginia, USA, that were stored at −20°C and thawed before use. These species were selected because they were locally available and represented a wide range of angiosperm taxonomic diversity that may correspond to variations in physical properties and secondary metabolite composition. Three leaves each of *C. dentata*, *L. tulipifera*, *A. rubrum*, and *Q. montana* were collected. Half of each leaf was used for FUSE, and the other half was used for control methods (Appendix S1). Three samples were acquired from each half. The tissue samples were prepared and processed under the experimental conditions described below.

FUSE pulse generation

A custom 32-element 500 kHz array transducer with a geometric focus of 75 mm, an aperture size of 150 mm, and an effective f-number of 0.58 was used for all experiments in this study (Kim et al., 2014). A custom high-voltage (~1 kV/element) pulser was used to drive the transducer and generate a short single-cycle ultrasound pulse. This short pulse length results in low duty cycles (typically <1%) and, combined with the impedance of the
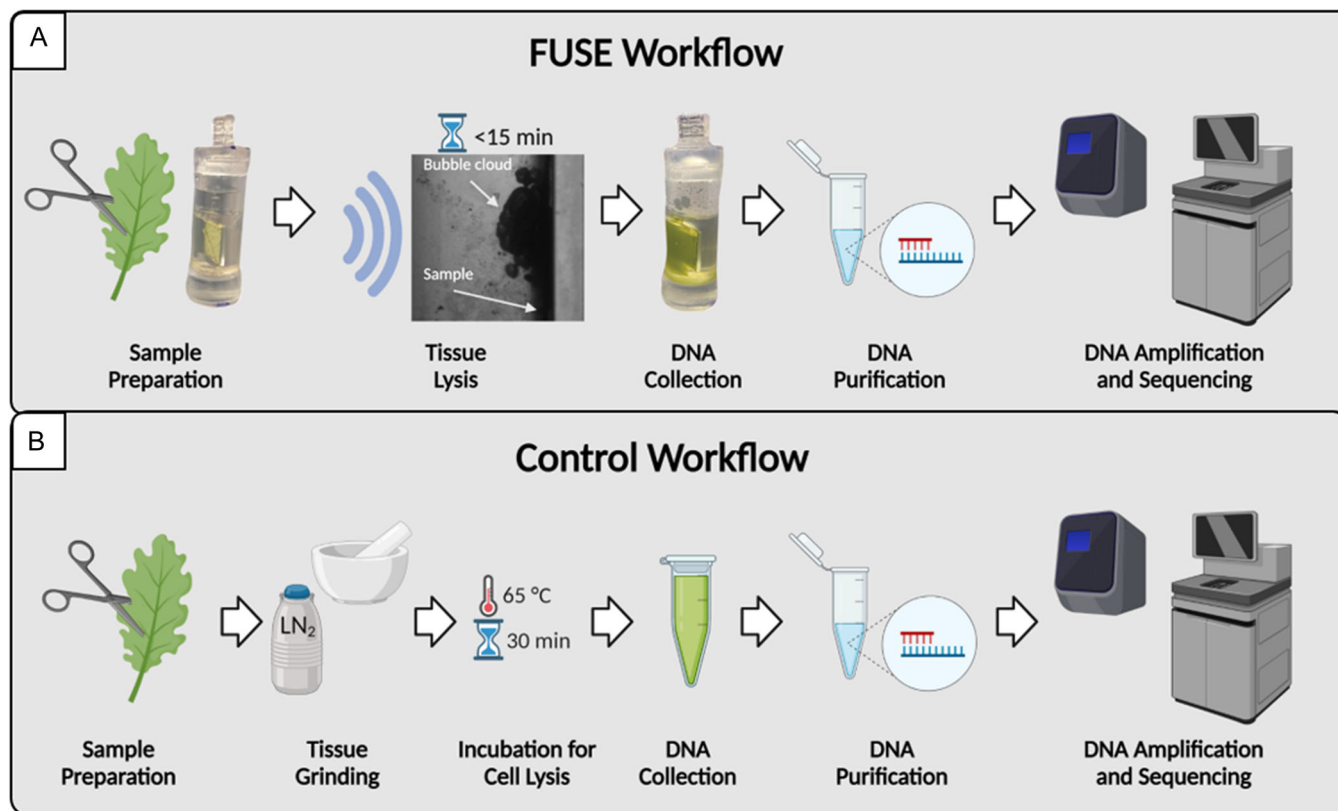
FIGURE 1 Comparison of the DNA extraction workflows. (A) The FUSE process begins with the trimming of leaf samples to prepare for tissue processing. The prepared sample is aligned with the cavitation bubble cloud. The tissue is disrupted, and cells are lysed in 15 min or less, eliminating the need for incubation. The DNA is then collected and purified for amplification and sequencing. (B) In the control extraction protocol, leaf samples are trimmed in preparation for tissue processing. Tissue processing involves manual grinding under liquid nitrogen for tissue breakdown and a 30-min minimum incubation period for cell lysis. The DNA is then collected and purified for amplification and sequencing following the same protocol as FUSE.

transducers, results in power requirements on the order of milliwatts that can be efficiently and safely supported by battery-powered electronics, even with the voltage driving requirements. The pulser was connected to a field-programmable gate array (FPGA) board (Altera DE0-Nano; Terasic Incorporated, Hsinchu, Taiwan), which was explicitly programmed for histotripsy therapy pulsing. A custom-built fiber-optic probe hydrophone (FOPH) (Parsons et al., 2006) was used to measure the acoustic peak negative output pressure ($p-$) of the transducers. The FOPH was cross-calibrated at low-pressure values ($p- < 2$ MPa) using a reference hydrophone (Onda HNR-0500; Onda Corporation, Sunnyvale, California, USA) to ensure accurate pressures were measured from the FOPH. The lateral and axial full-width half-maximum (FWHM) dimensions at the geometric focus of the transducer were measured to be 2.3 mm and 7.1 mm, respectively. The acoustic pressures used for all experiments were measured in degassed water at the focal point of the transducer, which was identified using a 3D beam scan. The acoustic output could not be directly measured at higher pressure levels ($p- > 16$ MPa) due to cavitation at the fiber tip. These pressures were estimated by summating the output focal $p-$ values from individual transducer elements.

Visualization of FUSE tissue disintegration

For all focused ultrasound experiments, high-speed optical imaging was performed using a machine-vision camera (Black-fly S 3.2MP Mono USB3 Vision; FLIR Integrated Imaging Solutions, Richmond, British Columbia, Canada) that was aligned with the focal zone of the transducer using a 100 mm F2.8 Macro lens (Tokina AT-X Pro; Kenko Tokina Co., Tokyo, Japan) and backlit by a custom-built pulsed LED strobe light capable of high-speed triggering with 1 μs exposures. As done in previous studies, the camera and the strobe light were triggered individually by the amplifier box, with the camera shutter opening at the time of pulse generation and the strobe acting as the shutter (Edsall et al., 2021a). The camera was triggered to capture one image every 50th pulse. The exposures were centered at delay times of 6, 48.5, and 98.5 μs after the pulse arrived at the focus to allow visualization of bubble cloud formation, coalescence, and collapse.

FUSE sample preparation and experimental configuration

All samples processed with FUSE were prepared as 12 mm squares using a sterile scalpel blade. The mass of the samples

ranged from 10–30 mg. Leaf samples were secured in a custom-designed sample holder that supported a 12.5 mm × 12.5 mm × 1 mm sapphire glass window, the leaf sample, and a polyethylene terephthalate glycol (PETG) square frame that secured the sample on the surface of the glass backing. The assembled sample holder was placed inside an optically transparent and acoustically permeable tube with an inner diameter of 9.525 mm and a wall thickness of 1.59 mm (Tygon PVC E-1000; McMaster-Carr, Elmhurst, Illinois, USA). When placed in the tube, cylindrical appendages at the top and bottom of the sample holder created a controlled volume chamber. The upper appendage featured a small circular opening for the application of lysis buffer into the chamber. The lysis buffer was composed of 1 mL of 1% PVP-40 Buffer AP1 solution and 8 μL of RNase A (Qiagen DNeasy Plant Kit; Qiagen, Hilden, Germany). A custom-built mount suspended the tube assembly in the water tank for tissue processing, and a stopper was designed to seal the other end of the tube. A robotic positioning system controlled by custom MATLAB scripts (Math-Works, Natick, Massachusetts, USA) was used to align samples with the focus of the ultrasonic transducer (Figure 2).

The configuration of the sample and sapphire glass backing in the focus of the transducer was chosen to maximize the efficiency of tissue sonication with FUSE. When ultrasonic pulses generate a cavitation bubble cloud near a rigid boundary, high-pressure collapse is expected to occur toward the surface of the boundary (Reisman

et al., 1998; Ikeda et al., 2006; Ma et al., 2018); this effect is demonstrated in Appendix S2. As the time after pulse arrival increased, microbubble coalescence became more evident, and the concentration of bubbles near the sample surface increased. Sapphire glass was chosen because it is hydrodynamically strong and has a high acoustic impedance. The hydrodynamic strength of the sapphire glass provided an unyielding surface to support the sample when exposed to high-pressure fluid flow caused by cavitation. The high acoustic impedance increased the pressure near the boundary and induced the cavitation bubbles to grow larger and collapse more violently. Overall, this effect maximized the impact pressure felt by the sample. In preliminary experiments, FUSE was tested without including the sapphire glass backing and sample holder. With this configuration, the sample was free to move outside of the focal zone, which decreased the tissue disintegration efficiency of FUSE and caused inconsistencies in tissue breakdown success.

FUSE tissue disintegration and DNA extraction

The prepared leaf tissue samples ($n = 9$) were processed using single-cycle ultrasound pulses delivered at a pressure of 34 MPa and a pulse repetition frequency (PRF) of 500 Hz. These pulse parameters, particularly the PRF, were selected following preliminary tissue breakdown experiments that revealed this to be the most time-efficient pulsing regime
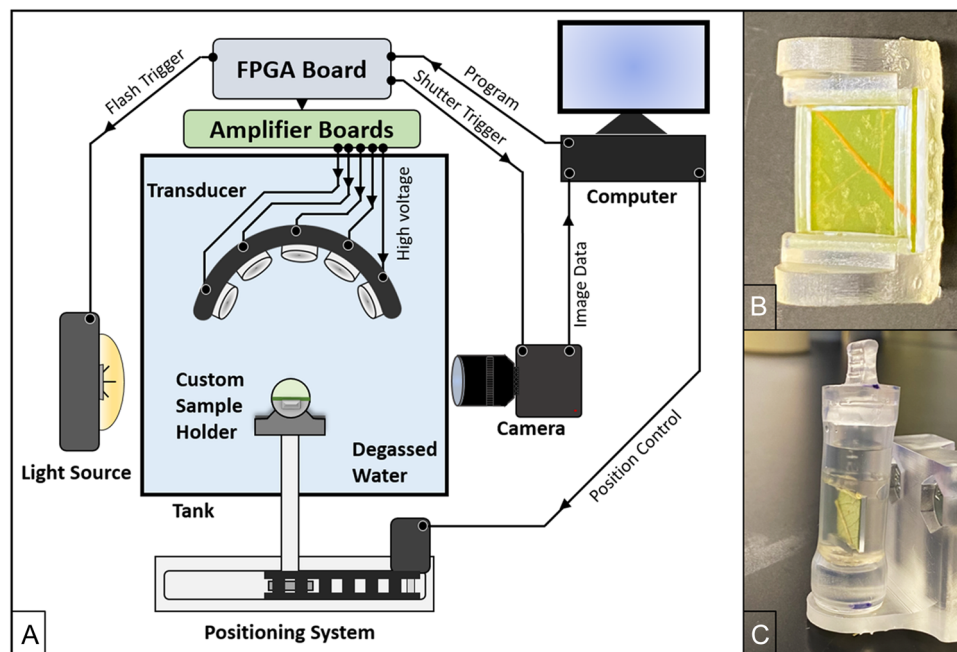

FIGURE 2 Experimental FUSE setup. (A) Ultrasonic transducers are driven by an FPGA board and amplifier. High-speed imaging is performed using a strobe and camera controlled by signals from the FPGA board. Custom scripts are delivered to the FPGA board, and imaging data are recorded by a computer. A robotic positioning system, controlled by the computer using MATLAB, is used to align the sample in the focus of the transducer array. (B) A custom sample holder designed to support a sapphire glass backing, the leaf sample, and a PETG frame is used. (C) The sample holder assembly is housed in an acoustically permeable tube for DNA extraction experiments.

before residual cavitation shield effects were observed. This effect is discussed further below, under "DNA extraction feasibility." Measurements made with a fiber optic hydrophone demonstrated that pressure loss was negligible (<1%) when pulses were delivered through the sample tube. Before tissue processing, the acoustic focus was directed at the center of the sample. To completely disintegrate the leaf tissue sample, MATLAB scripts controlling the positioning system were designed to move the sample in a spiral square pattern such that each point within the $100 \, mm^2$ disintegration zone was exposed to the focal bubble cloud for 0.5 s. Using this approach, a single scan of the applied pattern delivered 250 pulses per point, with multiple scans used for each sample to achieve sufficient tissue breakdown. After FUSE tissue disintegration and cell lysis, sample purification was performed in silica columns using the standard protocol as recommended by the manufacturer (Qiagen DNeasy Plant Kit).

The number of scans required for complete tissue disintegration was initially characterized for *C. dentata*, *L. tulipifera*, *A. rubrum*, and *Q. montana* samples ($n = 3$) backed with sapphire glass suspended in an open water bath. Images of the sample were taken after each scan. Each image was converted to grayscale, then to binary using the Otsu method (Otsu, 1979). The targeted tissue area was mapped as a region of interest (ROI) with dimensions of 10×10 mm to represent the area exposed to ultrasonic pulses. The disrupted tissue area inside and outside the ROI was quantified by counting the number of pixels using custom MATLAB scripts; pixel counts were then converted to tissue disintegration area. The significance of the area measurements was determined using an unpaired Student's *t*-test with unequal variance. Values less than 0.05 ($P < 0.05$) were considered significant.

Control sample tissue disintegration and DNA extraction

Control samples ($n = 9$) were obtained by cutting the leaf tissue into 100 mg segments, and samples were disrupted by grinding with mortar and pestle under liquid nitrogen (Westbrook et al., 2020). The control samples were put in the mortar, and liquid nitrogen was added to freeze the samples and cool the mortar, pestle, and spatula. To begin, samples were ground slowly with the pestle; once the liquid nitrogen was mostly evaporated, more vigorous grinding was performed to reduce the tissue to a fine powder. The tissue powder was then transferred to a 1.5 mL centrifuge tube where 1% PVP-40 Buffer AP1 solution and RNase A were added (Qiagen DNeasy Plant Kit). The lysis buffer volume varied depending on the quality of the leaf tissue sample, which was determined by assessing the sample's color and age. For older samples with a dark green or brown-green color, 1 mL of 1% PVP-40 Buffer AP1 solution and 8 µL of RNase A (0.8 mg) were used. For younger samples with a yellow-green color, 500 µL of 1% PVP-40

Buffer AP1 solution and 4 µL of RNase A (0.4 mg) were used. This was done because the leaves with a lower water content yielded a larger sample volume after grinding with mortar and pestle under liquid nitrogen and therefore required a greater buffer volume for proper cell lysis. After the addition of the buffer, cell lysis was carried out with an initial vortex of the tube to homogenize the solution before incubation at 65°C for 30 min with a short vortex every 5 min. Subsequent sample purification was performed in silica columns using the standard protocol as recommended by the manufacturer (Qiagen DNeasy Plant Kit).

DNA quantification

The robustness of FUSE was investigated by quantifying the released DNA. FUSE and control lysates were analyzed using a Qubit 4 Fluorometer (Thermo Fisher Scientific, Waltham, Massachusetts, USA) and a NanoDrop One (Thermo Fisher Scientific) to determine the quantity and quality of DNA released with FUSE and control samples. The DNA yield was reported as the quantity of DNA released per milligram of tissue to normalize input sample mass using the DNA concentration values from the Qubit. Lysates were also visualized using gel electrophoresis to assess DNA fragmentation. For data acquired from the NanoDrop and Qubit measurements, an unpaired Student's *t*-test with unequal variance was used, with values less than 0.05 ($P < 0.05$) considered significant.

Library preparation and PCR amplification

To compare the two methods for downstream genotyping, genotyping-by-sequencing (GBS) was performed on *C. dentata* genomic DNA extracted by FUSE and control methods. Library preparation involved restriction digestion followed by ligation of sequencing adapters and PCR amplification (Westbrook et al., 2020). *Castanea dentata* samples processed with FUSE and control methods were normalized to 55 ng, then digested with 1 µL of ApeKI (New England Biolabs, Ipswich, Massachusetts, USA). This restriction enzyme recognizes a 5 bp degenerate sequence GCWGC, where W is an A or T (Elshire et al., 2011). For one of the *C. dentata* samples processed with FUSE, the quantity of eluted DNA did not reach 55 ng, so 36.2 ng of DNA was used in the digestion reaction. The restriction fragment ligation was performed as described in previous studies (Westbrook et al., 2020). Briefly, the DNA fragments were ligated to Illumina-compatible adapters with 1.6 µL of T4 DNA ligase. P1 adapters contained a unique barcode region for each adapter immediately upstream of the ligated DNA fragment, and the P2 adapter was consistent for all samples. PCR amplification of the ligated fragments was performed using the primers and protocol reported previously (Elshire et al., 2011). The thermal cycling conditions were as follows: 95°C for 1 min, followed by 18

cycles of 95°C for 30 s, 63°C for 20 s, and 68°C for 30 s. Lastly, samples were brought to 68°C for 5 min and kept at 4°C. Ligation and amplification were assessed by gel electrophoresis and viewed with a 2100 Bioanalyzer instrument (Agilent, Santa Clara, California, USA) for all samples to determine if FUSE processing affected DNA integrity in a manner that impacted library preparation. DNA samples were purified before and after PCR using the Monarch PCR and DNA Clean-Up Kit (New England Biolabs). Individual sample libraries were pooled, and fragments ranging from 250–550 bp were selected using BluePippin (Sage Science, Beverly, Massachusetts, USA). The resulting library was visualized using a 2100 Bioanalyzer instrument.

Sequencing analysis

The *C. dentata* GBS libraries were sequenced using the NovaSeq 6000 instrument (Illumina, San Diego, California, USA) in 2×150 bp paired-end mode at the Duke University Center for Genomic and Computational Biology. Raw FASTQ files were demultiplexed and quality filtered with the STACKS process_radtags function. Specifically, reads were trimmed of provided adapter sequences, and removed if they either lacked an intact restriction cut site or had a mean quality score ≤10 over more than 15% (in this case, 23 bp) of their length (Catchen et al., 2013). Filtered reads were aligned to v.1.1 of the *C. dentata* reference genome (National Center for Biotechnology Information [NCBI] taxonomy ID: 134033) using the Burrows–Wheeler Aligner (BWA) mem algorithm and subsequently converted to BAM format with SAMtools (Westbrook et al., 2020). Heterozygous sites were called with the Genome Analysis Toolkit (GATK) HaplotypeCaller algorithm (McKenna et al., 2010; Poplin et al., 2018), and these genomic variant call formats (GVCFs) were then merged using the GenotypeGVCFs function. Variants were flagged and removed as low quality if they had the following characteristics: low map quality (MQ < 40); high strand bias (FS > 40); differential map quality between reads supporting the reference and alternative alleles (MQRankSum < −12.5); bias between the reference and alternate alleles in the position of alleles within the reads (ReadPosRankSum < −8.0); and low depth of coverage (DP < 5). Coverage depth per sample was calculated using the SAMtools depth function. Statistical analysis of coverage depth was performed using a Wilcoxon rank-sum test with values less than 0.05 ($P < 0.05$) considered significant.

RESULTS AND DISCUSSION

FUSE tissue disintegration

The feasibility of FUSE for leaf tissue disintegration was examined with *C. dentata*, *L. tulipifera*, *A. rubrum*, and *Q.* *montana* leaves by characterizing tissue breakdown after each FUSE scan (Figure 3A). For all species, the damaged tissue area increased as the number of scans increased, but the number of scans required to achieve significant tissue breakdown differed among species. *Liriodendron tulipifera* leaves were the most vulnerable to breakdown, as they were the only species with notable tissue disintegration after one scan. For *C. dentata*, *L. tulipifera*, and *A. rubrum* samples, tissue breakdown beyond the bounds of the targeted disintegration zone was observed. This effect was likely due to dispersed cavitation occurring outside the focal point of the converging pressure fronts. Surface inhomogeneities at solid–liquid interfaces result in the growth of cavitation nuclei that can induce cavitation at thresholds below the intrinsic threshold (Atchley and Prosperetti, 1989; Mørch, 2015). Previous work has also shown that leaves are more susceptible to cavitation-induced tissue disruption when gas channels are present in the tissue (Miller, 1977, 1983). Therefore, it is possible that the surface architecture and distribution of gas channels within the tissue matrices created cavitation nucleation sites outside the targeted area. It is also possible that residual gas bubbles from preceding pulses diffused outside the focus and served as cavitation nuclei. This would induce cavitation below the intrinsic pressure threshold and expose a larger area of the leaves to cavitation (Xu et al., 2006). Lastly, off-target leaf tissue disintegration could result from acoustic shielding, such that the residual bubbles in the acoustic focus increased the likelihood of acoustic scattering (Pishchalnikov et al., 2006; Maeda et al., 2018). The trends in tissue breakdown for *Q. montana* differed from the other three species (see below). It is expected that variation in tissue breakdown across species was due to differences in physical properties, such as water content and tissue strength.

The observed efficiency of FUSE tissue disintegration was assessed quantitatively by plotting the disintegration area inside the targeted region and the total disintegration area as a function of scan number (Figure 3B, C). The initial breakdown occurred the most rapidly in *L. tulipifera* leaves, as after the first scan $38.4 \pm 11.4\%$ of the targeted tissue region was disintegrated. In comparison, <10% of the target tissue was disintegrated after the first scan for *C. dentata*, *A. rubrum*, and *Q. montana*. The targeted *L. tulipifera* tissue region was significantly processed after two scans ($P < 0.05$ compared to zero scans). The initial breakdown of *C. dentata* leaves did not occur as rapidly as *L. tulipifera*, but *C. dentata* quickly approached complete tissue breakdown, as these leaves were significantly processed after three scans ($P < 0.05$ compared to zero scans). *Acer rubrum* leaves were more resistant to breakdown than *L. tulipifera* and *C. dentata*, as four scans were required to achieve significant breakdown ($P < 0.05$ compared to zero scans). Although *L. tulipifera*, *C. dentata*, and *A. rubrum* samples achieved significant breakdown in less than six scans, increasing the number of scans decreased the margin of error in the disintegration area. Therefore, six scans were used to process *C. dentata*, *L. tulipifera*, and *A. rubrum* samples to
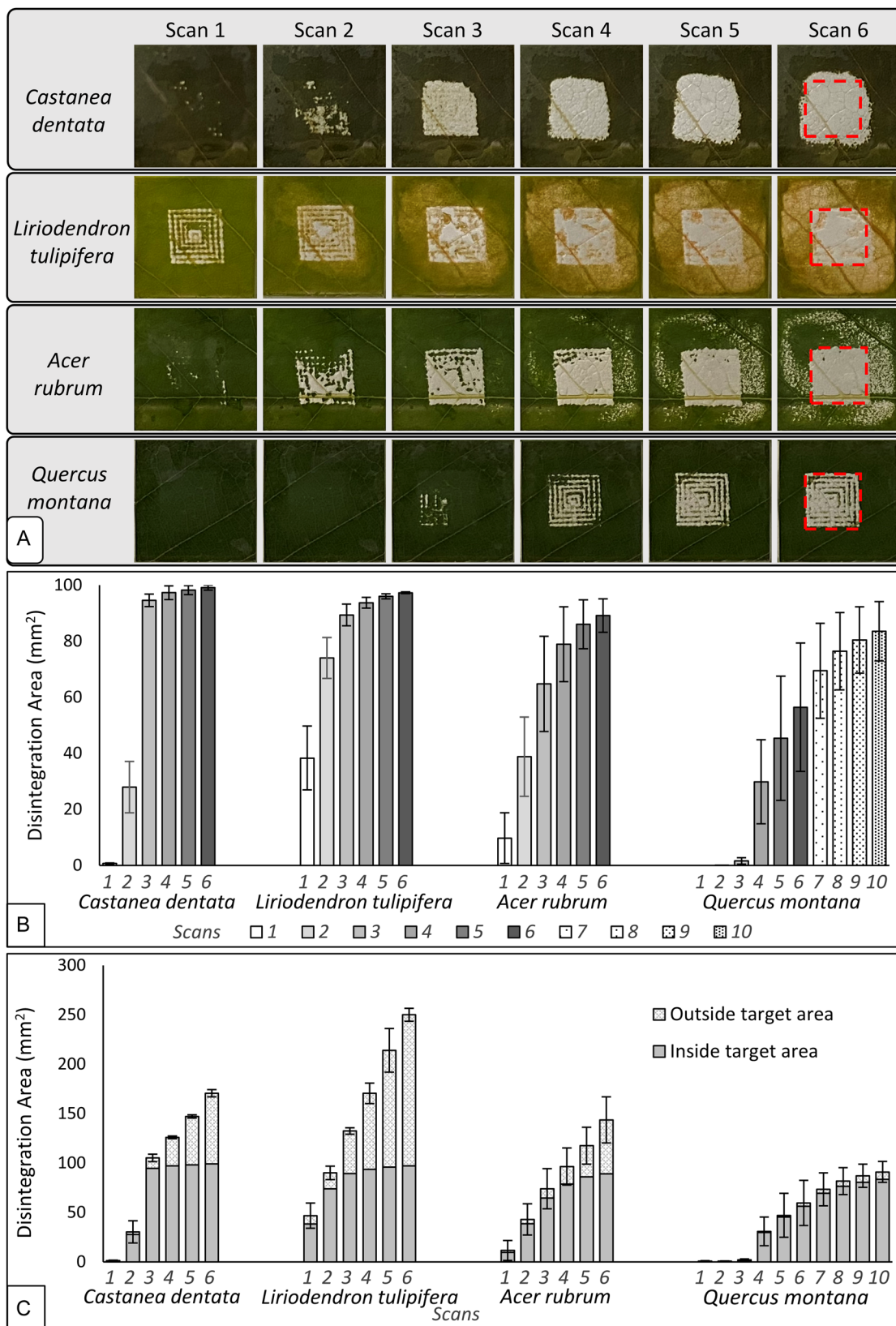
FIGURE 3 (A) Leaf tissue disintegration increases after each FUSE scan. The red square in the top right identifies the targeted tissue region. Tissue breakdown beyond the target area is the result of peripheral cavitation damage. The image data suggest that the leaf species affect FUSE tissue disintegration efficiency. (B) The disintegration area within the target area increases after each scan for all species. (C) The total disintegration area shows that tissue outside of the target area is also disintegrated by FUSE. Six scans are used for processing *Castanea dentata*, *Liriodendron tulipifera*, and *Acer rubrum* samples. *Quercus montana* samples required 10 scans for processing due to a reduction in disintegration efficiency.

allow more consistent comparisons. Six scans resulted in a 9-min tissue processing time and a total of 1500 pulses per point. *Quercus montana* was the most resistant to breakdown, as these samples required eight scans to achieve a significant breakdown ($P < 0.05$ compared to zero scans). Because increasing the scan number increased the area of disintegration and reduced the margin of error in the disintegration area, 10 scans were used for *Q. montana* tissue processing, resulting in a 15-min tissue processing time and 2500 pulses per point.

Leaf tissue breakdown outside of the targeted area was also quantified to examine the effects of dispersed cavitation. Trends in tissue breakdown outside of the targeted area were comparable to those observed within the targeted area, such that the tissue disintegration area increased as the number of scans increased. Additionally, the extent of *C. dentata*, *L. tulipifera*, and *A. rubrum* tissue disintegration outside the targeted region was greater than *Q. montana*. These results suggest that differences in the physical properties among leaf species also affect the extent of collateral tissue breakdown. However, collateral tissue breakdown is not of central importance for this study because the samples are restricted to the size of the targeted region in DNA extraction experiments.

DNA extraction feasibility

The determined number of FUSE scans required to disintegrate each leaf species was applied for DNA extraction experiments to characterize the quantity of DNA released by FUSE compared to the control protocol (Figure 4). Overall, FUSE was able to release greater quantities of DNA than control methods in a fraction of the processing time. Notably, FUSE increased the DNA yield with less than half of the input sample mass required by the control protocol. The quantity of DNA released with FUSE and the control protocol varied by species. The DNA yield provided by six FUSE scans was significantly greater than the control protocol for the *C. dentata* and *A. rubrum* samples. No significant differences were observed in the quantity of DNA released from *L. tulipifera* samples between six FUSE scans and the control protocol. For *Q. montana* leaves, the DNA yield provided by 10 FUSE scans was significantly greater than six FUSE scans and the control protocol, showing that the capacity of FUSE to release DNA from tough tissues improves with an increased number of processing scans.

The control protocol applied manual grinding under liquid nitrogen for tissue disruption and the Qiagen DNA extraction kit for cell lysis and DNA purification. Other tissue disruption techniques (e.g., homogenizers, rotor–stator mixers, blenders, or bead beaters) and DNA extraction techniques (e.g., CTAB-based methods) have also been used for DNA extraction from leaf tissue (Vincelli and Amsden, 2013). Here, mortar and pestle grinding under liquid nitrogen for tissue disruption and the Qiagen DNA extraction kit were used in the control protocol to provide an initial point of reference to demonstrate the feasibility of FUSE for leaf DNA extraction. Further research is needed to investigate the utility of FUSE compared to other conventional DNA extraction protocols.

The DNA yield results suggest that FUSE is as effective at DNA extraction as the control methods. Appendices S3–6
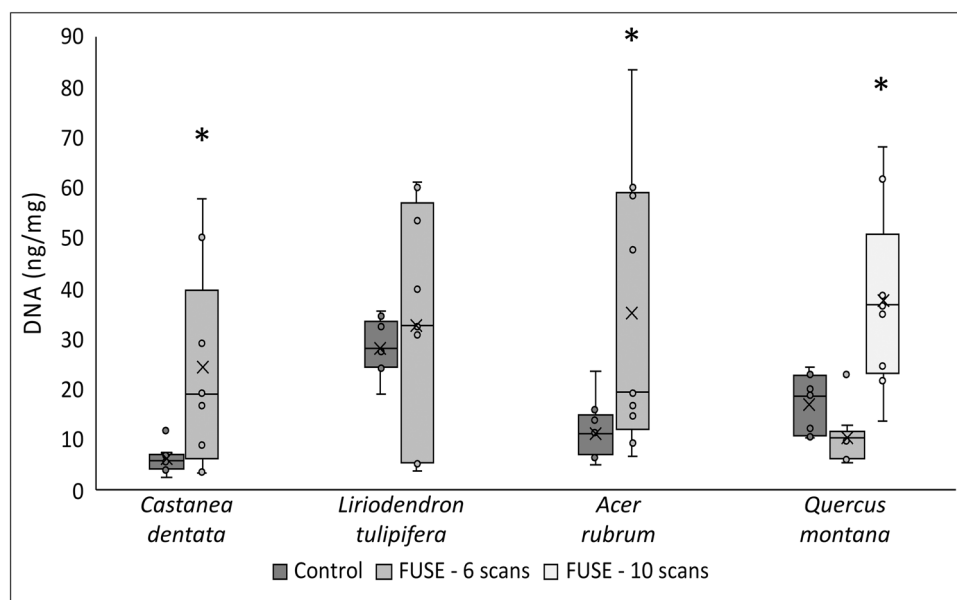

FIGURE 4 DNA extraction results show that FUSE releases DNA from leaf tissue. A significant increase in DNA release from *Castanea dentata* and *Acer rubrum* samples is observed when processed with six FUSE scans compared to controls. DNA release from *Quercus montana* samples is significantly higher when 10 FUSE scans are used for processing than controls. After six FUSE scans, DNA release from *Liriodendron tulipifera* samples is comparable to controls. *Indicates significant ($P < 0.05$) differences between FUSE and control samples.

include images of the leaf samples after FUSE processing to demonstrate the relationship between FUSE tissue disintegration and DNA release for each species. The results suggest that the degree of tissue disintegration influenced the concentration of DNA release for samples processed with FUSE. Therefore, it is likely that inconsistencies in tissue breakdown efficiency were a source of variation in the FUSE DNA yield results. The tissue disruption outside the targeted area observed in Figure 3 suggests the leaf tissue was seeding cavitation, which may be the result of bubble nuclei persisting on leaf tissue particles and causing effects similar to particle-mediated histotripsy (Edsall et al., 2021b). These residual bubble nuclei on the tissue surface could have influenced the behavior of subsequent pressure fronts and altered the cavitation efficacy at the acoustic focus, leading to inconsistencies in the efficiency of tissue breakdown and the DNA yield. Despite the observed variability in leaf tissue disintegration and DNA yield, the DNA extraction results confirm that FUSE can effectively release DNA from leaf tissue at quantities comparable to control protocols. However, variability in the results presents a need for further cavitation kinetics research to improve the consistency of FUSE processing.

The DNA extraction results show that leaf species influenced the DNA yield. Because the leaves chosen represented a range of angiosperm taxonomic diversity, it was expected that differences in physical and chemical properties would affect the quantity of DNA released. The control DNA yield data were examined to determine the effect of species on DNA release. The *C. dentata* DNA yield was significantly lower than the average DNA yield from the control samples, whereas the *L. tulipifera* DNA yield was significantly greater than the average DNA yield from the control samples. The *C. dentata* leaves were the only samples described as brown-green (Appendix S3), while the *L. tulipifera* leaves were the only samples characterized as yellow-green (Appendix S4). These sample characteristics suggest that the *C. dentata* samples were more mature than the *L. tulipifera* samples at the time of collection (Goralka et al., 1996). It is common for older leaves to have greater amounts of secondary metabolites, which often cause low yield and poor-quality DNA (Porebski et al., 1997). Therefore, it is likely that the age of the sampled leaves was a factor in the observed inconsistencies in the quantity of the released DNA. Different leaf tissue types such as frozen, lyophilized, or herbarium specimens could be used to investigate the effect of leaf degradation on DNA release with FUSE. Tissue is often frozen, lyophilized, or stored as herbarium specimens to reduce tissue degradation and allow for long-term storage. As greater DNA yield was observed from samples with less degradation, we expect that FUSE can be applied to frozen, lyophilized, or herbarium specimens, but may require some additional preparation, such as pre-soaking to rehydrate the tissue, and further research is necessary to confirm the applicability of other leaf tissue types.

The 260/280 and 260/230 ratios were measured to assess the quality of the DNA extracted with FUSE and control methods (Table 1). For *C. dentata* and *Q. montana*, the 260/280 ratio was significantly higher for samples processed with six FUSE scans than for control samples, whereas for *A. rubrum* the 260/280 ratio for six FUSE scans was significantly lower than control methods. No discernible trends were observed in 260/230 ratios, with values in the expected range for leaf tissue. However, the 260/230 ratio was significantly higher after 10 FUSE scans than control methods for *Q. montana* leaves. This significant difference is expected to be the result of increased tissue breakdown releasing more carbohydrates from the leaf tissue. Some species processed with FUSE showed high standard error in 260/230 ratios. This result is likely due to incomplete tissue disintegration for some samples within these groups.

The FUSE protocol used in this work involves a non-thermal tissue lysis process that has been shown to reduce the time required for DNA release (Holmes et al., 2020). The acoustic parameters used in this study, particularly the PRF of 500 Hz, were chosen for this initial feasibility study based on preliminary tissue breakdown experiments. In previous work, Atlantic salmon muscle tissue was processed with FUSE using 10,000 pulses delivered at 25 Hz, which resulted in a total processing time of 6 min and 40 s (Holmes et al., 2020). In this study, 270,000 pulses were applied at 500 Hz to complete six FUSE scans, and 450,000 pulses were applied at 500 Hz to complete 10 FUSE scans, resulting in total processing times of 9 and 15 min, respectively. At 500 Hz PRF, the time efficiency of FUSE was improved without inducing thermal effects. However, further increasing the PRF is likely to result in cavitation

TABLE 1 The quality of DNA released by FUSE is comparable to DNA released by control methods. FUSE requires less processing time than control methods and releases greater quantities of DNA. DNA quantification measurements are reported from Qubit fluorometer measurements, and 260/280 and 260/230 ratios are reported from NanoDrop measurements.

| Sample type	FUSE				Control methods			
	Time (min:s)	DNA (ng/mg)	260/280	260/230	Time (min:s)	DNA (ng/mg)	260/280	260/230
Castanea dentata	9:00	24.33 ± 6.51	2.34 ± 0.31	2.68 ± 3.51	30:00	6.22 ± 0.87	1.45 ± 0.01	0.52 ± 0.01
Liriodendron tulipifera	9:00	32.61 ± 7.82	1.77 ± 0.05	1.41 ± 0.34	30:00	28.37 ± 1.78	1.83 ± 0.01	1.99 ± 0.06
Acer rubrum	9:00	35.32 ± 9.21	1.63 ± 0.04	1.95 ± 0.60	30:00	11.51 ± 1.95	1.85 ± 0.02	2.53 ± 0.19
Quercus montana (6 scans)	9:00	10.65 ± 1.74	1.84 ± 0.11	0.17 ± 3.00	30:00	17.17 ± 1.98	1.52 ± 0.01	0.66 ± 0.02
Quercus montana (10 scans)	15:00	37.85 ± 5.93	1.76 ± 0.03	2.28 ± 0.20	30:00	17.17 ± 1.98	1.52 ± 0.01	0.66 ± 0.02
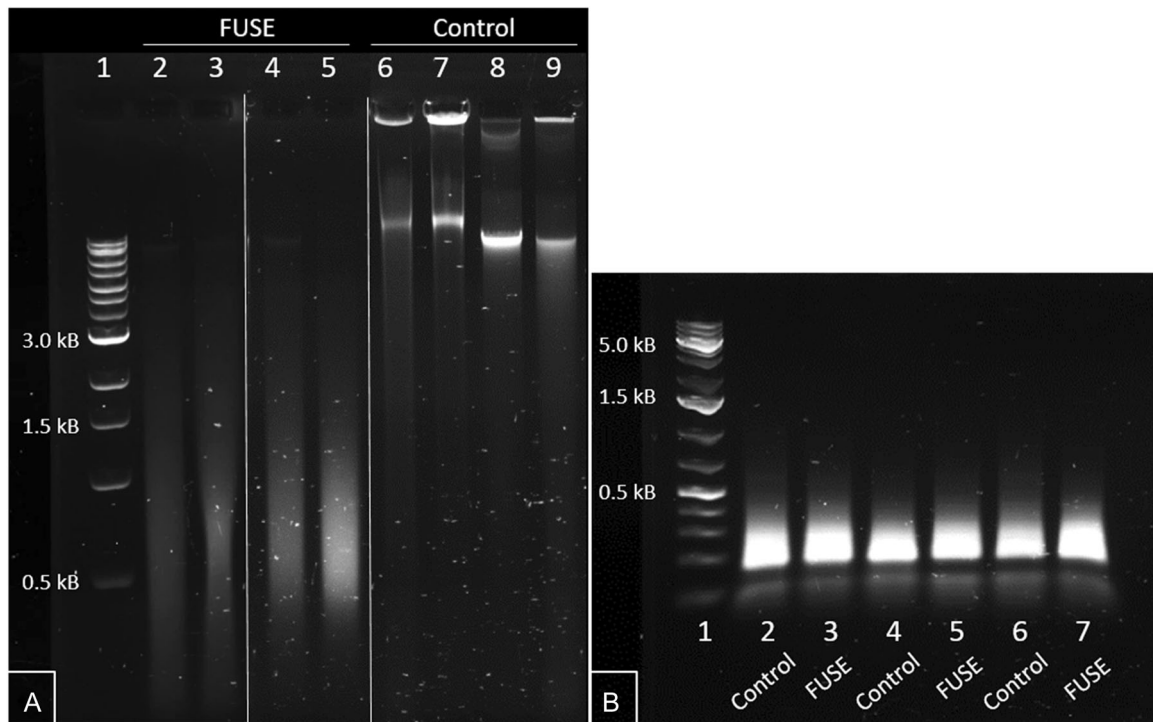
FIGURE 5 (A) Visualization of DNA extracts resulting from FUSE and control methods shows that FUSE fractionates large genomic DNA fragments. (B) The genomic DNA fractionation facilitated by FUSE did not affect GBS library preparation. Note that Gel A contains images from different parts of the same gel; the rearrangements are marked with white lines.
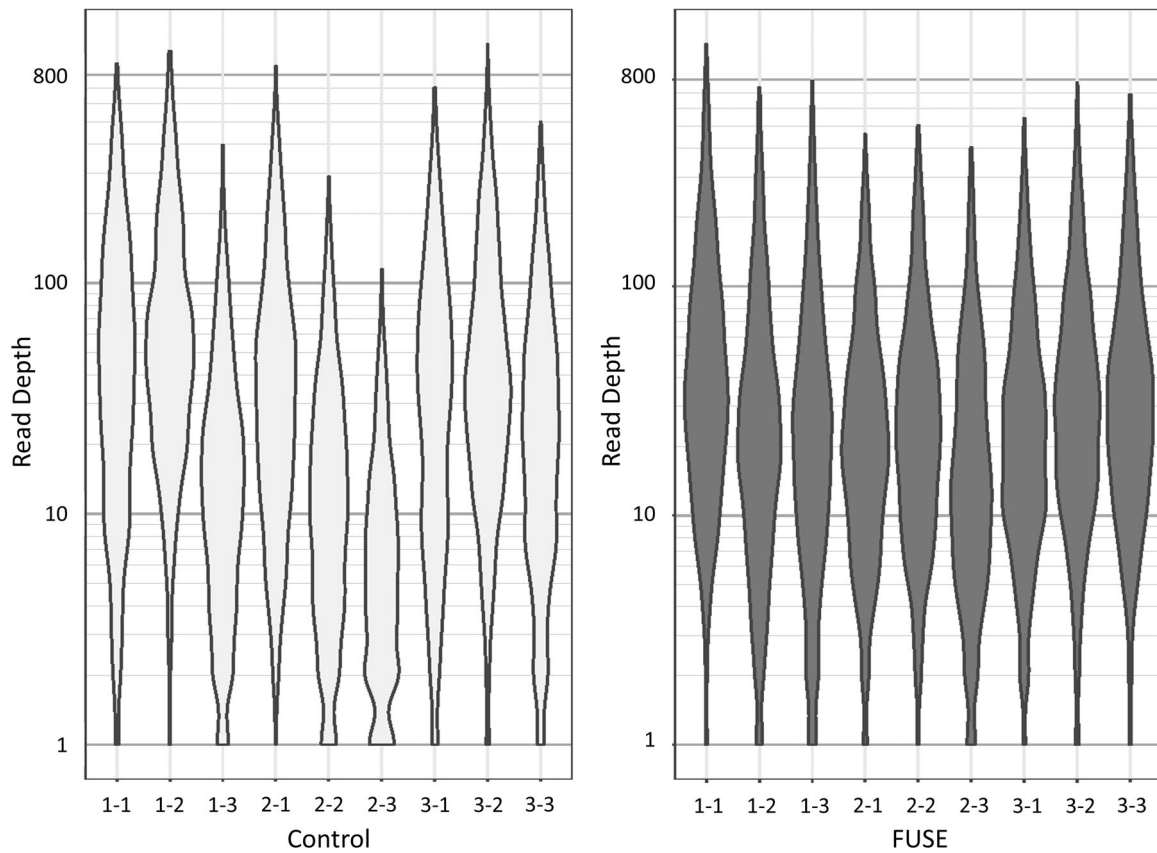

FIGURE 6 FUSE provides DNA suitable for short-read next-generation sequencing. The uniformity of read depth across conventional and FUSE samples is comparable. The *x*-axis labeling represents the leaf and sample number, such that 1-2 identifies the read depth for leaf 1, sample 2.

shielding effects that lower the effectiveness of each pulse (Pishchalnikov et al., 2006; Maeda et al., 2018), so future work will be necessary to explore the optimal pulsing parameters for the implementation of higher PRFs. The optimization of pulsing parameters to implement FUSE at higher PRFs will allow FUSE to be applied to more robust tissue types that require more pulses for tissue breakdown without increasing the tissue processing time.

DNA amplification

Castanea dentata samples were selected for amplification and sequencing. The samples processed with FUSE and control methods amplified successfully, demonstrating that FUSE can yield high-quality DNA from leaf tissue suitable for PCR amplification. A subset of the amplified DNA lysates and libraries was visualized using gel electrophoresis (Figure 5) and a 2100 Bioanalyzer instrument (Appendix S7). Visualization of the lysates shows that large genomic DNA fragments were fractionated by FUSE processing, but no differences in the prepared GBS libraries were observed.

Sequencing

All *C. dentata* samples processed with FUSE and control methods provided high-quality next-generation sequencing reads (GenBank accession number: PRJNA837224). Because downstream applications of this technology are expected to be focused on identifying genetic variants from sequence data for population genetics and systematics, we estimated read depth for variable sites, which showed that FUSE samples had a depth comparable to controls. Read depth was moderately correlated between the two extraction methods (Appendix S8), and mean depth was not significantly different (25.7 for FUSE and 27.1 for controls; $P = 0.155$ based on a Wilcoxon rank-sum test) (Figure 6). Overall, these results indicate that FUSE processing is suitable for short-read next-generation sequencing analysis. Observations of large DNA fragment fractionation may suggest further optimization of FUSE may be necessary to enable long-read sequencing. However, these results demonstrate the need for future studies investigating the underlying mechanisms of DNA fragmentation under FUSE processing.

CONCLUSIONS

This study assessed the efficacy of our recently developed FUSE protocol in plant tissues by testing samples from *C. dentata*, *L. tulipifera*, *A. rubrum*, and *Q. montana* leaves. The success of the FUSE protocol was determined by visualizing the extent of tissue breakdown observed after FUSE sonication, measuring the quantity and quality of the released DNA, and evaluating the suitability of the resulting DNA extracts for short-read sequencing. PCR amplification and next-generation sequencing were performed to determine if the quality of the DNA was acceptable for these analyses. In accordance with previous work that established the effectiveness of FUSE for releasing DNA from Atlantic salmon muscle tissue (Holmes et al., 2020), the results of this study demonstrate that FUSE can provide high quantities of DNA suitable for amplification and short-read sequencing in less time than conventional plant extraction methods that apply grinding under liquid nitrogen for tissue disruption and the Qiagen DNA extraction kit. Additionally, these results suggest that the input sample mass required by FUSE is less than what is necessary for the control extraction methods applied in this study, which could be advantageous in future work that aims to develop field-deployable FUSE systems for conservation efforts. Overall, this study shows that the applications of FUSE can be extended to plant tissue, a robust tissue that is more resistant to mechanical breakdown and has a chemical composition that has made DNA accessibility more challenging (Porebski et al., 1997; Rachmayanti et al., 2009; Särkinen et al., 2012). In conjunction with previous findings (Holmes et al., 2020), these results suggest that FUSE could be used as a novel platform for DNA extraction capable of accelerating workflows for a variety of sample types.

AUTHOR CONTRIBUTIONS
A.S., H.H., A.M., and E.V. developed the methodology for focused ultrasound experiments. Q.Z. and J.H. developed and performed the methodology for PCR and next-generation sequencing experiments. A.S., I.M., and Q.Z. gathered the data. A.S., H.H., Q.Z., J.H., and M.W. analyzed the data from molecular experiments. A.S., H.H., A.M., and E.V. analyzed data from focused ultrasound experiments. A.S. led the writing of the manuscript. All authors contributed critically to the drafts and approved the final version of the manuscript.

DATA AVAILABILITY STATEMENT
All genetic sequences generated in this work are available on GenBank. Next-generation sequencing data can be accessed with the accession number PRJNA837224.

ORCID

Alexia Stettinius https://orcid.org/0000-0001-6499-5797
Hal Holmes https://orcid.org/0000-0001-7534-4463
Eli Vlaisavljevich https://orcid.org/0000-0002-4097-6257

REFERENCES

Atchley, A. A., and A. Prosperetti. 1989. The crevice model of bubble nucleation. *Journal of the Acoustical Society of America* 86: 1065–1084.

Bader, K. B., E. Vlaisavljevich, and A. D. Maxwell. 2019. For whom the bubble grows: Physical principles of bubble nucleation and dynamics in histotripsy ultrasound therapy. *Ultrasound in Medicine and Biology* 45: 1056–1080.

Buser, J. R., X. Zhang, S. Byrnes, P. Ladd, E. Heiniger, M. Wheeler, J. Bishop, et al. 2016. A disposable chemical heater and dry enzyme preparation for lysis and extraction of DNA and RNA from microorganisms. *Analytical Methods* 8: 2880–2886.

Catchen, J., P. A. Hohenlohe, S. Bassham, A. Amores, and W. A. Cresko. 2013. Stacks: An analysis tool set for population genomics. *Molecular Ecology* 22: 3124–3140.

Cornwell, W. K., W. D. Pearse, R. L. Dalrymple, and A. E. Zanne. 2019. What we (don't) know about global plant diversity. *Ecography* 42: 1819–1831.

Dormontt, E. E., M. Boner, B. Braun, G. Breulmann, B. Degen, E. Espinoza, S. Gardner, et al. 2015. Forensic timber identification: It's time to integrate disciplines to combat illegal logging. *Biological Conservation* 191: 790–798.

Edsall, C., E. Ham, H. Holmes, T. L. Hall, and E. Vlaisavljevich. 2021a. Effects of frequency on bubble-cloud behavior and ablation efficiency in intrinsic threshold histotripsy. *Physics in Medicine & Biology* 66: 225009.

Edsall, C., Z. M. Khan, L. Mancia, S. Hall, W. Mustafa, E. Johnsen, A. L. Klibanov, et al. 2021b. Bubble cloud behavior and ablation capacity for histotripsy generated from intrinsic or artificial cavitation nuclei. *Ultrasound in Medicine and Biology* 47: 620–639.

Elshire, R. J., J. C. Glaubitz, Q. Sun, J. A. Poland, K. Kawamoto, E. S. Buckler, and S. E. Mitchell. 2011. A robust, simple genotyping-by-sequencing (GBS) approach for high diversity species. *PLoS ONE* 6: e19379.

Finch, K. N., F. A. Jones, and R. C. Cronn. 2019. Genomic resources for the Neotropical tree genus *Cedrela* (Meliaceae) and its relatives. *BMC Genomics* 20: 58.

Finch, K. N., R. C. Cronn, M. C. Ayala Richter, C. Blanc-Jolivet, M. C. Correa Guerrero, L. De Stefano Beltrán, C. R. García-Dávila, et al. 2020. Predicting the geographic origin of Spanish Cedar (*Cedrela odorata* L.) based on DNA variation. *Conservation Genetics* 21: 625–639.

Goralka, R. J., M. A. Schumaker, and J. H. Langenheim. 1996. Variation in chemical and physical properties during leaf development in California bay tree (*Umbellularia californica*): Predictions regarding palatability for deer. *Biochemical Systematics and Ecology* 24: 93–103.

CBOL Plant Working Group. 2009. A DNA barcode for land plants. *Proceedings of the National Academy of Sciences, USA* 106: 12794–12797.

Halewood, M., T. Chiurugwi, R. Sackville Hamilton, B. Kurtz, E. Marden, E. Welch, F. Michiels, et al. 2018. Plant genetic resources for food and agriculture: Opportunities and challenges emerging from the science and information technology revolution. *New Phytologist* 217: 1407–1419.

Holliday, J. A., S. N. Aitken, J. E. K. Cooke, B. Fady, S. C. González-Martínez, M. Heuertz, J.-P. Jaramillo-Correa, et al. 2017. Advances in ecological genomics in forest trees and applications to genetic resources conservation and breeding. *Molecular Ecology* 26: 706–717.

Holmes, H. R., M. Haywood, R. Hutchison, Q. Zhang, C. Edsall, T. L. Hall, D. Baisch, et al. 2020. Focused ultrasound extraction (FUSE) for the rapid extraction of DNA from tissue matrices. *Methods in Ecology and Evolution* 11: 1599–1608.

Ikeda, T., S. Yoshizawa, M. Tosaki, J. S. Allen, S. Takagi, N. Ohta, T. Kitamura, and Y. Matsumoto. 2006. Cloud cavitation control for lithotripsy using high intensity focused ultrasound. *Ultrasound in Medicine and Biology* 32: 1383–1397.

Jain, M., H. E. Olsen, B. Paten, and M. Akeson. 2016. The Oxford Nanopore MinION: Delivery of nanopore sequencing to the genomics community. *Genome Biology* 17: 239.

Jiao, L., M. Yu, A. C. Wiedenhoeft, T. He, J. Li, B. Liu, X. Jiang, and Y. Yin. 2018. DNA barcode authentication and library development for the wood of six commercial *Pterocarpus* species: The critical role of xylarium specimens. *Scientific Reports* 8: 1945.

Kersey, P. J. 2019. Plant genome sequences: Past, present, future. *Current Opinion in Plant Biology* 48: 1–8.

Kim, Y., A. D. Maxwell, T. L. Hall, Z. Xu, K.-W. Lin, and C. A. Cain. 2014. Rapid prototyping fabrication of focused ultrasound transducers. *IEEE Transactions on Ultrasonics, Ferroelectrics, and Frequency Control* 61: 1559–1574.

Liu, Y., C. Xu, Y. Sun, X. Chen, W. Dong, X. Yang, and S. Zhou. 2021. Method for quick DNA barcode reference library construction. *Ecology and Evolution* 11: 11627–11638.

Ma, J., C.-T. Hsiao, and G. L. Chahine. 2018. Numerical study of acoustically driven bubble cloud dynamics near a rigid wall. *Ultrasonics Sonochemistry* 40: 944–954.

Maeda, K., A. D. Maxwell, T. Colonius, W. Kreider, and M. R. Bailey. 2018. Energy shielding by cavitation bubble clouds in burst wave lithotripsy. *Journal of the Acoustical Society of America* 144: 2952–2961.

Mancia, L., E. Vlaisavljevich, Z. Xu, and E. Johnsen. 2017. Predicting tissue susceptibility to mechanical cavitation damage in therapeutic ultrasound. *Ultrasound in Medicine and Biology* 43: 1421–1440.

McKenna, A., M. Hanna, E. Banks, A. Sivachenko, K. Cibulskis, A. Kernytsky, K. Garimella, et al. 2010. The Genome Analysis Toolkit: A MapReduce framework for analyzing next-generation DNA sequencing data. *Genome Research* 20: 1297–1303.

Miller, D. L. 1977. The effects of ultrasonic activation of gas bodies in *Elodea* leaves during continuous and pulsed irradiation at 1 MHz. *Ultrasound in Medicine and Biology* 3: 221–240.

Miller, D. L. 1983. The botanical effects of ultrasound: A review. *Environmental and Experimental Botany* 23: 1–27.

Mørch, K. A. 2015. Cavitation inception from bubble nuclei. *Interface Focus* 5: 20150006.

Niemz, A., T. M. Ferguson, and D. S. Boyle. 2011. Point-of-care nucleic acid testing for infectious diseases. *Trends in Biotechnology* 29: 240–250.

Otsu, N. 1979. A threshold selection method from gray-level histograms. *IEEE Transactions on Systems, Man, and Cybernetics* 9: 62–66.

Parsons, J. E., C. A. Cain, and J. B. Fowlkes. 2006. Cost-effective assembly of a basic fiber-optic hydrophone for measurement of high-amplitude therapeutic ultrasound fields. *Journal of the Acoustical Society of America* 119: 1432–1440.

Pironon, S., J. S. Borrell, I. Ondo, R. Douglas, C. Phillips, C. K. Khoury, M. B. Kantar, et al. 2020. Toward unifying global hotspots of wild and domesticated biodiversity. *Plants* 9: 1128.

Pishchalnikov, Y. A., J. A. McAteer, M. R. Bailey, I. V. Pishchalnikova, J. C. Williams, Jr., and A. P. Evan. 2006. Acoustic shielding by cavitation bubbles in shock wave lithotripsy (SWL). *AIP Conference Proceedings* 838: 319–322. https://doi.org/10.1063/1.2210369

Poplin, R., V. Ruano-Rubio, M. A. DePristo, T. J. Fennell, M. O. Carneiro, G. A. Van der Auwera, D. E. Kling, et al. 2018. Scaling accurate genetic variant discovery to tens of thousands of samples. BioRxiv 201178 [Preprint] [posted 24 July 2018]. Available at https://doi.org/10.1101/201178 [accessed 22 December 2022].

Porebski, S., L. G. Bailey, and B. R. Baum. 1997. Modification of a CTAB DNA extraction protocol for plants containing high polysaccharide and polyphenol components. *Plant Molecular Biology Reporter* 15: 8–15.

Rachmayanti, Y., L. Leinemann, O. Gailing, and R. Finkeldey. 2009. DNA from processed and unprocessed wood: Factors influencing the isolation success. *Forensic Science International: Genetics* 3: 185–192.

Reisman, G., Y.-C. Wang, and C. E. Brennen. 1998. Observations of shock waves in cloud cavitation. *Journal of Fluid Mechanics* 355: 255–283.

Särkinen, T., M. Staats, J. E. Richardson, R. S. Cowan, and F. T. Bakker. 2012. How to open the treasure chest? Optimising DNA extraction from herbarium specimens. *PLoS ONE* 7(8): e43808.

Small, R. L., J. A. Ryburn, R. C. Cronn, T. Seelanan, and J. F. Wendel. 1998. The tortoise and the hare: Choosing between noncoding plastome and nuclear *Adh* sequences for phylogeny reconstruction in a recently diverged plant group. *American Journal of Botany* 85: 1301–1315.

Vincelli, P., and B. Amsden. 2013. Comparison of tissue-disruption methods for PCR-based detection of plant pathogens. *Plant Disease* 97: 363–368.

Vlaisavljevich, E., A. Maxwell, L. Mancia, E. Johnsen, C. Cain, and Z. Xu. 2016. Visualizing the histotripsy process: Bubble cloud–cancer cell interactions in a tissue-mimicking environment. *Ultrasound in Medicine and Biology* 42: 2466–2477.

Westbrook, J. W., Q. Zhang, M. K. Mandal, E. V. Jenkins, L. E. Barth, J. W. Jenkins, J. Grimwood, et al. 2020. Optimizing genomic selection for blight resistance in American chestnut backcross populations: A trade-off with American chestnut ancestry implies resistance is polygenic. *Evolutionary Applications* 13: 31–47.

Xu, Z., J. B. Fowlkes, and C. A. Cain. 2006. A new strategy to enhance cavitational tissue erosion using a high-intensity, initiating sequence. *IEEE Transactions on Ultrasonics, Ferroelectrics, and Frequency Control* 53: 1412–1424.

Xu, Z., T. L. Hall, E. Vlaisavljevich, and F. T. Lee, Jr. 2021. Histotripsy: The first noninvasive, non-ionizing, non-thermal ablation technique based on ultrasound. *International Journal of Hyperthermia* 38: 561–575.

SUPPORTING INFORMATION

Additional supporting information can be found online in the Supporting Information section at the end of this article.

Appendix S1. Leaf sample allocation. Each leaf used in this study was divided into two, providing a matched pair to compare FUSE and conventional extraction yields.

Appendix S2. Progression of cavitation bubble cloud collapse toward the surface of the leaf tissue.

Appendix S3. *Castanea dentata* tissue breakdown and DNA yield results. DNA quantification measurements are reported from Qubit fluorometer measurements, and 260/280 and 260/230 ratios are reported from NanoDrop measurements.

Appendix S4. *Liriodendron tulipifera* tissue breakdown and DNA yield results. DNA quantification measurements are reported from Qubit fluorometer measurements, and 260/280 and 260/230 ratios are reported from NanoDrop measurements.

Appendix S5. *Acer rubrum* tissue breakdown and DNA yield results. DNA quantification measurements are reported from Qubit fluorometer measurements, and 260/280 and 260/230 ratios are reported from NanoDrop measurements.

Appendix S6. *Quercus montana* tissue breakdown and DNA yield results. DNA quantification measurements are reported from Qubit fluorometer measurements, and 260/280 and 260/230 ratios are reported from NanoDrop measurements.

Appendix S7. Visualization of DNA libraries with a Bioanalyzer. The resultant DNA libraries for samples prepared with control methods (A) are comparable to samples prepared with FUSE (B).

Appendix S8. Relationship between $\log_{10}$ sequencing depth at variable sites with FUSE and control samples.